Wave-vector dependence of magnetic properties of excitons in ZnTe

L. C. Smith, J. J. Davies,* and D. Wolverson
Department of Physics, University of Bath, Bath BA2 7AY, United Kingdom

H. Boukari and H. Mariette
CEA-CNRS Group Nanophysique et Semiconducteurs, Institut Néel-CNRS/Université Joseph Fourier, 25 Rue des Martyrs, 38042 Grenoble, France

V. P. Kochereshko
A.F. Ioffe Physico-Technical Institute, RAS, 194021 St. Petersburg, Russia

R. T. Phillips
Cavendish Laboratory, J.J. Thomson Avenue, Cambridge CB3 0HE, United Kingdom
(Received 19 January 2011; published 18 April 2011)

The magnetic properties of heavy-hole excitons in wide quantum wells of ZnTe with $Zn_xMg_{1-x}Te$ barriers have been studied with photoluminescence and reflectivity measurements. The exciton magnetic moments (as characterized by the g values) and the diamagnetic shifts of the exciton transitions are found to depend strongly on the wave-vector component K_z associated with translational motion of the exciton normal to the plane of the quantum well. The case of ZnTe differs from examples of this behavior previously reported for GaS, CdTe, and ZnSe since the ZnTe is under tensile biaxial strain, so that the heavy-hole exciton states lie higher in energy than the corresponding states of the light-hole excitons. The dependence of the magnetic properties on K_z is nevertheless still in excellent agreement with the predictions of a model proposed by Smith *et al.* [Phys. Rev. B **78**, 085204 (2008)], in which mixing of the heavy-hole 1S exciton state with light-hole nP states is found to be responsible for motion-induced changes in the internal structure of the exciton.

DOI: 10.1103/PhysRevB.83.155206 PACS number(s): 71.35.Cc, 71.35.Ji, 78.20.Ls, 78.55.Et

I. INTRODUCTION

The properties of excitons in bulk semiconductors can conveniently be described by using the center-of-mass (c.m.) approximation, in which the exciton is considered as a composite particle formed by the electron and hole orbiting each other (the internal motion), with the center of mass moving with translational wave vector $\vec{K}$ (see, e.g., Refs. 1–5). When such excitons are created in quantum wells that are wide (for example, five or more times the exciton radius), the c.m. approximation remains valid, but the allowed values of the wave-vector component K_z in the growth direction (taken to be the z axis) are now discrete and in an infinitely deep well of width L are given by $K_z = N\pi/L$, with corresponding kinetic energies of $h^2N^2/8ML^2$, where M is the translational mass, N is the quantization index, and h is Planck's constant. These energies are typically of the order of millielectron volts and the transitions associated with the creation of excitons with different values of K_z can often be observed in high-resolution optical spectroscopy. Examples have been reported for several materials, notably CdTe,[6,7] GaAs, [8] ZnSe,[9] and ZnTe.[10]

Recent optical experiments in magnetic fields have shown, however, that the properties of excitons with finite translational wave vectors are more complicated than appears at first sight.[11–14] In particular, the exciton magnetic moment (characterized by its g value, g_{exc}) is found to be highly dependent on K_z, in some cases changing by an order of magnitude over the range of accessible values of K_z. The magnetic moment is sensitive to the electronic structure of the exciton, which itself is thus shown to depend on its state of motion. In Ref. 12 a model was proposed in which the changes in magnetic properties are caused by motion-induced mixing between the exciton states. The mixing is a consequence of the valence band structure departing from simple parabolic form, and the model leads to excellent agreement with observation for CdTe and ZnSe. In these two materials, the epitaxial nature of the specimens results in a strain-splitting S between the heavy-hole (HH) and light-hole (LH) exciton states, so that the heavy-hole exciton lies lowest in energy (S being positive). The heavy-hole exciton 1S ground state is then mixed with the *light*-hole nP states, leading to the observed changes in the magnetism.

Clearly, the extent of the mixing in this model would depend on the energy differences between the 1S heavy-hole state and the light-hole nP states, and these differences in turn depend in part on the strain in the epitaxial layers. Thus, to provide a clear indication that it is indeed the mixing of heavy- and light-hole exciton states that leads to the motion-induced changes in the magnetic properties, it is necessary to show that these changes are sensitive to the extent of the strain in the quantum well and to show that these changes can be accounted for quantitatively. To a limited degree it was possible to test this sensitivity in CdTe, where the layers were in biaxial compressive strain for which two different values could be obtained by growing on different types of substrate: one of the successes of the model was that it indeed accounted accurately for the consequent changes in the exciton magnetism.[12,14] However, only two values of the strain were possible and only for CdTe: in particular, the investigations did not include the possibility of biaxial *tensile* strain. Experiments

involving a much greater variation of the strain were therefore necessary in order to establish the general applicability of the model and to eliminate other possible mechanisms (for example, mixing between heavy-hole exciton states caused by high-order terms in the valence band Hamiltonian). The purpose of the present study on ZnTe was therefore to provide not merely a different material but also a case in which the biaxial strain, being tensile, was completely different from that in previously studied materials. To obtain this type of strain, the ZnTe layers were grown between $Zn_{1-x}Mg_xTe$ barriers (see Sec. II A): the parameter S is now *negative* (the lowest optically excited state now being that of the *light*-hole exciton).

The plan of the paper is as follows. We first provide the sample details and a summary of the optical spectra in magnetic fields (Sec. II). The anisotropy and K_z dependence of the gyromagnetic ratios and diamagnetic constants of the exciton are described in Sec. III. A comparison of the data with the model of Ref. 12 is made in Sec. IV, followed by our overall conclusions (Sec. V).

II. EXPERIMENTAL DETAILS

A. Sample details

The specimens were grown by molecular beam epitaxy on ZnTe (001) substrates. A bottom barrier of ~1100-nm $Zn_{1-x}Mg_xTe$ was grown on a 400-nm ZnTe buffer layer, followed by a ZnTe quantum well and an outer barrier of 50 nm of $Zn_{1-x}Mg_xTe$. Further details are given in Table I. Since the $Zn_{1-x}Mg_xTe$ has a larger lattice constant than ZnTe, the quantum wells are placed under biaxial tensile strain. The strain-splitting parameter S was obtained in each case from reflectivity spectra (see Sec. II B): the values of S are about one-half of those predicted by using the parameters of Ref. 15 and by assuming that the wells are fully strained to fully relaxed bottom barriers.

B. Spectra and energy shifts in magnetic fields

Photoluminescence (PL) and reflectivity experiments were carried out in the range 1.6 to 7 K and in magnetic fields up to 10 T. In most cases, the field was applied in the specimen growth direction ([001], the z axis), but some measurements were made with samples inclined to the magnetic field. PL spectra were excited by using the 442-nm He-Cd or 496-nm Ar-ion laser lines. In all measurements the direction of light propagation was along that of the magnetic field.

Typical examples of the spectra in zero magnetic field are shown in Fig. 1. We attribute the two strongest peaks (2.374 and 2.380 eV) in the PL spectrum to the $N = 1$ transitions of the light-hole and heavy-hole $1S$ excitons, respectively. Transitions associated with the heavy-hole center-of-mass

TABLE I. Details of the ZnTe/$Zn_{1-x}Mg_xTe$ samples

Sample number	L (nm)	x	S (±1 meV)
1($M1893$)	100	0.05	−5
2($M2097$)	80	0.05	−6
3($M2174$)	80	0.09	−9
4($M2175$)	50	0.09	−9

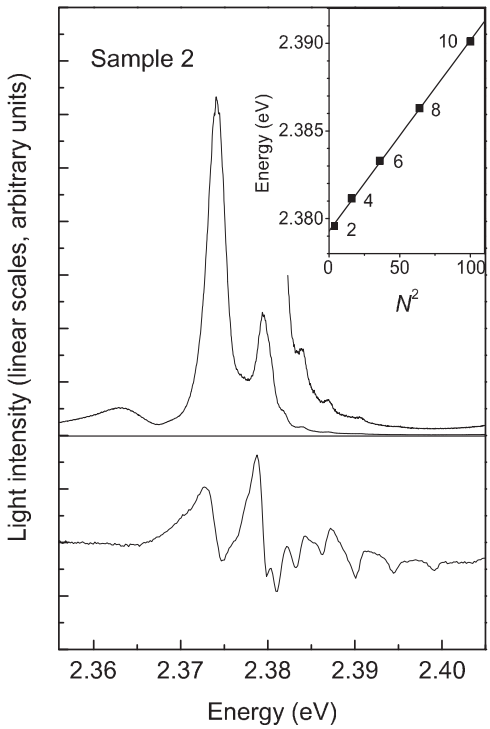

FIG. 1. Reflectivity (lower panel) and photoluminescence (upper panel) spectra from sample 2 ($L = 80$ nm, $S = -6$ meV) at 1.6 K in zero magnetic field. The inset shows the c.m. transition energies plotted against the square of the translational quantum number N, whose values are indicated in the diagram. For this value of L and for $N > 1$, the signals for even values of N are much stronger than those for odd values (see, e.g., Refs. 6 and 7).

excitons appear as a series of lines in the energy region 2.380 eV and above. When the energies of these transitions are plotted against the square of the quantization index they lie on a straight line of gradient $h^2/8ML^2$, with $M = 0.54m_0$ (see inset to Fig. 1). This value of the translational mass M is close to the sum $m_e + m_{HH}$ ($m_e = 0.166m_0$, $m_{HH} = 0.40m_0$ from the data in Ref. 16), thus confirming that the transitions are indeed those of HH c.m. excitons. For LH c.m. excitons, transitions with differing values of N cannot be identified with certainty (see also Sec. IV C).

When a magnetic field B is applied along the growth axis, the PL and reflectivity lines split and change in energy as typified in Fig. 2 where the continuous lines are of the form

$$E = E_N + DB^2 \pm g_{exc}\mu_B B/2 \qquad (1)$$

in which, for a given specimen, E_N, g_{exc}, and D are functions of N [in obtaining such spectra, the PL signals become progressively weaker as the energy increases (see, e.g., Fig. 1) and, since the degree of circular polarization is not perfect, discrimination between weak signals that overlap can become difficult, thus accounting for small discrepancies between the observed and fitted data such as those in the upper trace of Fig. 2].

It is immediately apparent that the field-induced splitting of the exciton lines increases as the quantization index increases, in a manner that is very similar to that observed for CdTe, GaAs, and ZnSe.[11–14] The splitting, which is linear in magnetic

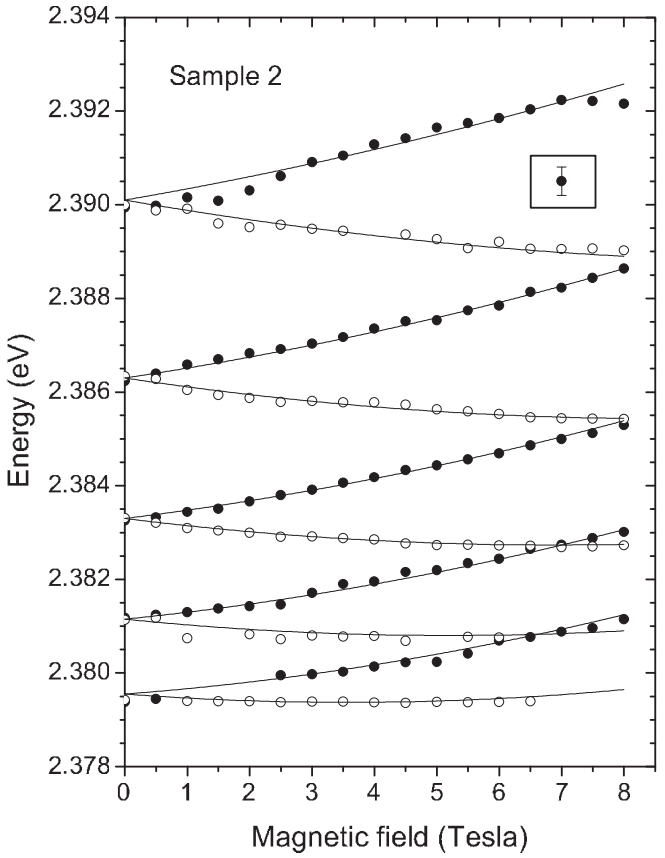

FIG. 2. The dependence of the transition energies of sample 2 as a function of magnetic field at 6.8 K. Filled and open symbols are for σ_+ and σ_- transitions, respectively. The continuous lines are of the form given by Eq. (1). The error bar indicated in the inset corresponds to the full width at half maximum of a typical signal.

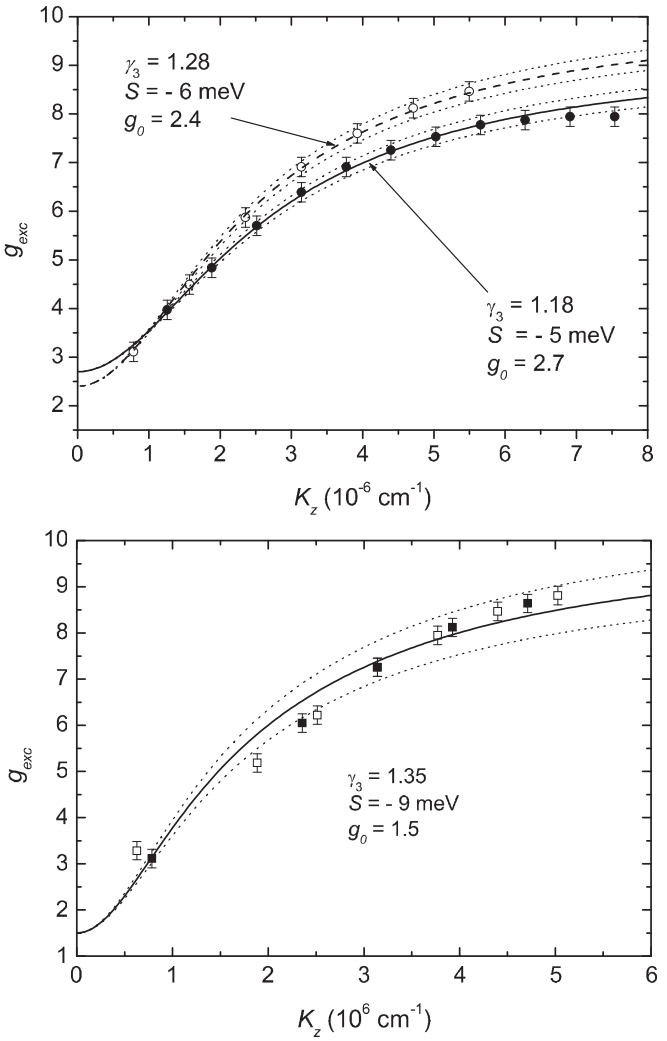

FIG. 3. Exciton g values as a function of the z component of the translational wave vector. The upper panel shows the data for the cases that the strain-splitting parameter $S = -5$ meV and $S = -6$ meV (filled circles and open circles are experimental data for samples 1 and 2, respectively). The lower panel shows the data for the case that the strain-splitting parameter $S = -9$ meV (filled and open squares are experimental data for samples 3 and 4, respectively). The curves are calculated as described in Sec. IV, with values of $\gamma_3 = 1.18 \pm 0.02$ (sample 1), $\gamma_3 = 1.28 \pm 0.02$ (sample 2), and $\gamma_3 = 1.35 \pm 0.05$ (samples 3 and 4). In each case, the curves shown by taking the outer values of the quoted error limits are shown by the dotted lines. The parameter g_0 is the value of $g_{\rm exc}$ at $K_z = 0$ and corresponds to $g_{\rm HH} - g_e$.

field, can be characterized by an exciton g value defined through $g_{\rm exc}\mu_B B = E_{\sigma+} - E_{\sigma-}$, where $E_{\sigma+}$ and $E_{\sigma-}$ are, respectively, the energies of the σ_+ and σ_- transitions and μ_B is the Bohr magneton.

III. ANISOTROPY AND K_z DEPENDENCES OF THE g FACTOR AND DIAMAGNETIC CONSTANTS OF THE EXCITON

It was pointed out in Refs. 11–14 that when the values of $g_{\rm exc}$ for quantum wells of different widths are plotted not against the quantization index but against the translational wave-vector component K_z, they lie on a common curve (for a given value of the strain parameter S). The data for the present samples plotted in this way are shown in Fig. 3.

The transitions, respectively, involve the heavy-hole exciton states with $m_J = \pm 3/2, m_s = \mp 1/2$, where m_J and m_s are, respectively, the magnetic quantum numbers for the hole and electron. It is convenient to express the exciton g value in terms of the heavy-hole g value ($g_{\rm HH}$),[17] the conduction band electron g value (g_e), and an additional parameter $g(K_z)$ that describes the effect of K_z-dependent mixing between the HH exciton $1S$ ground state and the excited LH states of nP form (see Sec. IV A). We therefore write

$$g_{\rm exc} = g_{\rm HH}\cos\theta - g_e + g(K_z)\cos\theta, \qquad (2)$$

where θ is the angle between the magnetic field and the growth axis. The $\cos\theta$ factor enters in the first term on the right-hand side because it is heavy holes that are involved (for which the in-plane g value is vanishingly small) and in the final term because $g(K_z)$ is predicted (see Sec. IV A) to have this form. In Fig. 4 we show the dependence on θ of two of the transitions, thus confirming the validity of Eq. (2) (and confirming that it is indeed heavy-hole excitons that are involved). The value of $g_e = -0.4 \pm 0.2$, which is expected to be essentially independent of the direction of the magnetic

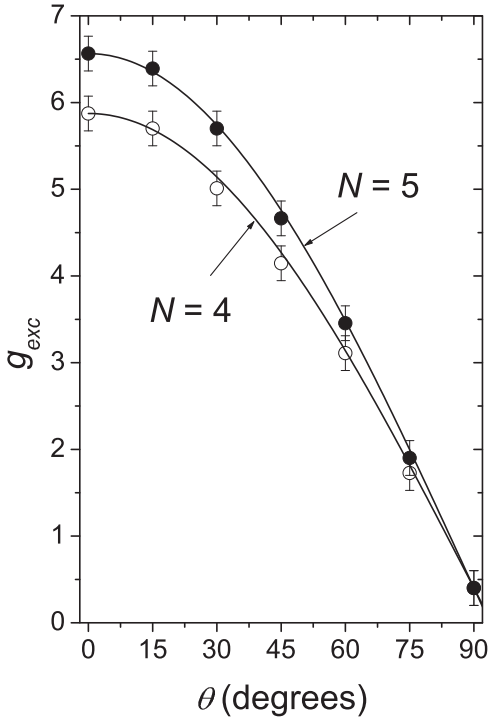

FIG. 4. Dependence of the exciton g value on the angle θ between the magnetic field and the growth axis for the $N = 4$ and $N = 5$ transitions in sample 1 ($L = 100$ nm, $S = -5$ meV). The curves are of the form given in Eq. (2).

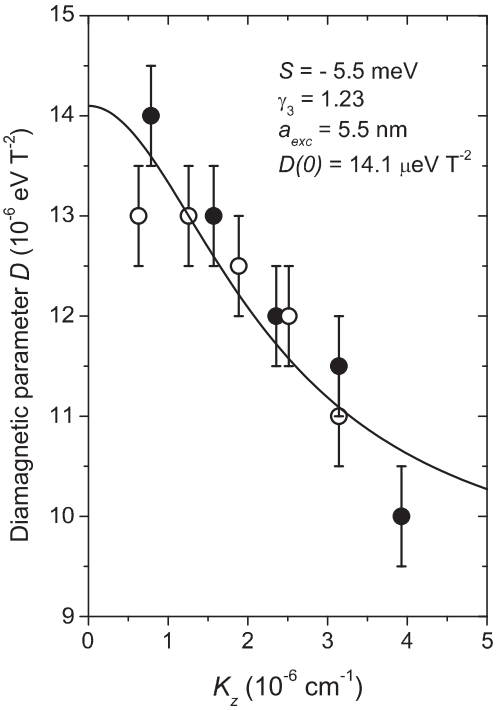

FIG. 5. The exciton diamagnetic parameter D as a function of the z component of the translational wave vector for samples 1 (filled circles) and 2 (open circles). The curve is calculated as described at the end of Sec. IV, with the strain-splitting parameter $S = -5.5$ meV taken to be the average for the two samples.

field, is consistent with the values of -0.4 and -0.78 given in Refs. 16 and 18.

The diamagnetic constant D [Eq. (1)] is also a function of the translational wave vector K_z, as shown in Fig. 5. Its behavior is discussed in Sec. IV B below.

IV. DISCUSSION

A. The *g* factor of the exciton

We interpret the data in terms of the model proposed in Ref. 12. Here, the $1S$ HH exciton state is mixed with the light-hole exciton states of nP form. The Luttinger Hamiltonian for holes in the valence band[3,19] contains a term of the form $-2\gamma_3 \frac{\hbar^2}{m_0}(\{k_x k_y\}\{J_x J_y\} + cycl.perm.)$ and it is this term that leads to the mixing[12]. For mixing with a particular nP light-hole exciton state, this results in a contribution to the exciton g-value given by:

$$\delta g_n = \left(\frac{24\gamma_3^2\hbar^2\beta^2\cos\theta}{m_0}\right)\left(\frac{v_n w_n}{\Delta E_n}\right)K_z^2. \quad (3)$$

Here $v_n = -\langle nP, p_x|\partial/\partial x|1S\rangle a_{\rm exc}$ and $w_n = \langle nP, p_x|x|1S\rangle a_{\rm exc}^{-1}$, where $a_{\rm exc}$ is the exciton Bohr radius. The parameter β represents the fraction of the translational momentum carried by the heavy hole and is defined by $\beta = m_{\rm HH}/(m_{\rm HH} + m_{\rm e})$, where $m_{\rm HH}$ and m_e are, respectively, the effective masses of the heavy holes and the conduction band electrons.

The quantity ΔE_n is the energy by which the nP LH state lies above the $1S$ HH state and is given by

$$\Delta E_n = R\left(1 - \frac{1}{n^2}\right) + S + \hbar^2\left(\frac{1}{2M_{\rm LH}} - \frac{1}{2M_{\rm HH}}\right)K_z^2, \quad (4)$$

where $M_{\rm LH}$ and $M_{\rm HH}$ are, respectively, the translational masses of LH and HH excitons, and where R is the exciton Rydberg energy [$R = 14.1$ meV (Ref. 16)].

For the particular case of $n = 2$, the values of v_2 and w_2 are $0.279a_{\rm exc}^{-1}$ and $0.745a_{\rm exc}$, respectively. For mixing with this particular state, and if $3R/4 + S$ is zero (or greater), the perturbation theory used to obtain Eq. (3) is valid, provided that $K_z >\sim w/a_{\rm exc} \approx 0.6 \times 10^6$ cm^{-1} (or less). This is indeed the case for the range of observation in the present study, especially since $3R/4 + S$ is positive (so that the $2P$ LH exciton state lies above the $1S$ HH state). For mixing with other nP states, the criterion is less demanding. To calculate $g(K_z)$, the contributions of the form of Eq. (3) have to be summed for all nP states and integrated over P-like states in the continuum.

Comparison between experiment and the predictions of this model are shown in Fig. 3 (upper panel) for samples 1 and 2. The Luttinger constants $\gamma_1 = 4.07$, $\gamma_2 = 0.78$ given in Ref. 16 have been used, together with $m_e = 0.116m_0$.[16] To fit the data we require $\gamma_3 = 1.18 \pm 0.02$ (sample 1) and $\gamma_3 = 1.28 \pm 0.02$ (sample 2); these values are lower than the value $\gamma_3 = 1.59$ in Ref. 16 but within the range reported in other studies (see Table II of Ref. 16). The only other adjustable parameter is g_0 (the heavy-hole exciton g value for notionally zero wave vector), the choice of which shifts the calculated curves bodily in a vertical direction in Fig. 3. A previous study of CdTe (Ref. 12) suggested that this parameter is strain dependent and, for ZnTe, we take $g_0 = 2.7 \pm 0.2$ for $S = -5$ meV and $g_0 = 2.4 \pm 0.2$ for $S = -6$ meV (leading, respectively, to values of 2.3 and 2.0 for $g_{\rm HH}$, the hole g value at $K_z = 0$).

The lower panel of Fig. 3 shows a similar fit to the data for samples 3 and 4 ($S = -9$ meV). Here we find $\gamma_3 = 1.35 \pm 0.05$ and $g_0 = 1.5$ (leading to $g_{\rm HH} = 0.1$), suggesting again a strain dependence of these parameters. The fit to the data is not as good as for the specimens with smaller strains, possibly because the perturbation theory is now being used closer to the limit of its applicability [see comment earlier in the section: the quantity $(3R/4 + S)$ is now close to zero]. However, given the approximations used, we consider the fit to be satisfactory.

We noted at the end of Sec. II B that the electron g value (obtained from the data point at $\theta = 90^\circ$) is negative (-0.4), in agreement with published data.[16,18] In contrast, the values of the HH g value needed to fit the present data are positive. This positive sign is a consequence (i) of extrapolating the experimental data for $g_{\rm exc}$ as K_z approaches the notional value of zero and (ii) of making the usual assumption that $g_{\rm exc}$ is then given by $g_{\rm HH} - g_e$ (this sign determination is not a consequence of the motion-induced mixing model, which itself concerns only the *range* over which $g_{\rm exc}$ varies as K_z changes). The positive sign is surprising, since $g_{\rm HH}$ is expected to be of the order -6 times the Luttinger parameter κ (Refs. 17 and 19) and since (for bulk ZnTe) values of κ ranging between zero and of 0.27 have been reported (see Table 1 of Ref. 16). At present, this difference in sign (and, indeed, the large variation in the value of κ reported for the bulk material) is not understood, but may be a consequence of the strain or of the differences in the state of binding of the hole. Attempts to calculate $g_{\rm HH}$ directly from knowledge of the band structure of ZnTe lie beyond the scope of the present paper.

B. The diamagnetic parameter of the exciton

We turn next to the behavior of the diamagnetic constant D as a function of translational wave vector (Fig. 5). It is shown in Ref. 12 that the mixing between the $1S$ and nP states results in contributions to the diamagnetic parameter $D(K_z)$ for $\theta = 0$ given by

$$\delta D(K_z) = -\frac{3}{2}\left(\frac{\gamma_3 \beta \hbar e a_{\rm exc}}{m_0}\right)^2 \left(\frac{w_n^2}{\Delta E_n}\right) K_z^2. \qquad (5)$$

As with the calculation of $g(K_z)$, these contributions to the diamagnetic parameter D have to be summed over all nP states. Since the contributions are negative, as K_z increases they will cause the value of $D(K_z)$ to fall below its value $D(0)$ for $K_z = 0$. In Fig. 5 we show the comparison between experiment and calculation for samples 1 and 2, using the average of the parameters used for the calculation for Fig. 3 (upper panel). We obtain good agreement with experiment if we choose $a_{\rm exc} = 5.5$ nm, which is a reasonable value for this material. [20]

C. The light holes

A final comment concerns the light-hole excitons. For small values of N and of the translational wave vector K_z the $1S$ LH exciton transitions lie lower in energy than those of the $1S$ HH excitons. The peak attributed to the $1S$ LH $N = 1$ transition appears strongly in, for example, Fig. 1, but we can find no conclusive evidence for LH transitions with higher values of N and therefore cannot obtain for these excitons a fan diagram of the type shown in Fig. 2. The predicted g value for LH excitons at small values of the translational wave vector is of order $g_e + g_{\rm LH} \approx g_e + g_{\rm HH}/3 \approx 0.5$ or less. This would not be resolvable in our spectra (particularly since the linewidth of the exciton LH signal is slightly greater than those for the exciton HHs).

V. CONCLUSIONS

The main conclusion is that the mixing model introduced in Ref. 12 to account for the wave-vector dependence of the heavy-hole g value remains valid even when it is the *light*-hole exciton ground state that is lowest in energy, that is, when the strain parameter S is negative. The excellent quantitative agreement that is obtained between the observed and the predicted values of the exciton g values and of the changes in the diamagnetic shifts provides further strong confirmation of the validity of the model, which implies that the internal structure of the exciton changes significantly as it acquires kinetic energy.

ACKNOWLEDGMENTS

We are grateful for support from the EPSRC-GB(UK) (Project No. EP/E025412), the CNRS, the Royal Society, the RFBR, and the Presidium RAS.

*j.j.davies@bath.ac.uk

[1] J. O. Dimmock, in *Semiconductors and Semimetals*, edited by R. K. Willardson and A. C. Beer (Academic, New York, 1967), Vol. 3, p. 259.

[2] M. Altarelli and N. O. Lipari, Phys. Rev. **7**, 3798 (1973).

[3] K. Cho, S. Suga, W. Deybrodt, and F. Willman, Phys. Rev. B **11**, 1512 (1975).

[4] E. L. Ivchenko and G. Pikus, *Superlattices and other Microstructures* (Springer-Verlag, Berlin, 1995).

[5] E. L. Ivchenko, *Semiconductor Nanostructures* (Alpha Science International, Harrow, United Kingdom, 2005).

[6] Y. Merle d'Aubigné, Le Si Dang, A. Wasiela, F. d'Albo, and A. Million, Journal de Physique Colloques **48**, 363 (1987).

[7] H. Tuffigo, R. T. Cox, N. Magnea, Y. Merle d'Aubigné, and A. Million, Phys. Rev. B **37**, 4310 (1988).

[8] A. Tredicucci, Y. Chen, F. Bassani, J. Massies, C. Deparis, and G. Neu, Phys. Rev. B **47**, 10348 (1993).

[9] S. Lankes, M. Meier, T. Reisinger, and W. Gebhardt, J. Appl. Phys. **80**, 4049 (1996).

[10] P. Lefebvre, V. Calvo, N. Magnea, T. Taliercio, J. Allègre, and H. Mathieu, Phys. Rev. B **56**, R10040 (1997).

[11] J. J. Davies, D. Wolverson, V. P. Kochereshko, A. V. Platonov, R. T. Cox, J. Cibert, H. Mariette, C. Bodin, C. Gourgon, E. V. Ubyivovk, Yu. P. Efimov, and S. A. Eliseev, Phys. Rev. Lett. **97**, 187403 (2006).

[12]L. C. Smith, J. J. Davies, D. Wolverson, S. Crampin, R. T. Cox, J. Cibert, H. Mariette, V. P. Kochereshko, M. Wiater, G. Karczewski, and T. Wojtowicz, Phys. Rev. B **78**, 085204 (2008).

[13]J. J. Davies, L. C. Smith, D. Wolverson, A. Gust, C. Kruse, D. Hommel, and V. P. Kochereshko, Phys. Rev. B **81**, 085208 (2010).

[14]J. J. Davies, L. C. Smith, D. Wolverson, V. P. Kochereshko, J. Cibert, H. Mariette, H. Boukari, M. Wiater, G. Karczewski, T. Wojtowicz, A. Gust, C. Kruse, and D. Hommel, Phys. Status Solidi B **247**, 1521 (2010).

[15]K. Watanabe, M. Th. Litz, M. Korn, W. Ossau, A. Waag, G. Landwehr, and U. Schüssler, J. Appl. Phys. **81**, 451 (1997).

[16]Ch. Neumann, A. Nöthe and N. O. Lipari, Phys. Rev. B **37**, 922 (1988).

[17]$g_{hh} = -6\kappa$ in the notation of Ref. 3.

[18]M. Willatzen, M. Cardona, and N. E. Christensen, Phys. Rev. B **51**, 17992 (1995).

[19]J. M. Luttinger, Phys. Rev. **102**, 1030 (1956).

[20]M. Fox in *Optical Properties of Solids* (Oxford University Press, Oxford, United Kingdom, 2010), 2nd ed., p. 97.